DOI: 10.1002/ejic.200601238

The Role of Equatorial and Axial Ligands in Promoting the Activity of Non-Heme Oxidoiron(IV) Catalysts in Alkane Hydroxylation

Leonardo Bernasconi,*[a] Manuel J. Louwerse,[a] and Evert Jan Baerends*[a]

Keywords: Density functional calculations / Fenton reaction / Alkanes / Hydroxylation / High-valent oxidoiron(IV) systems / Push effect

The key electronic structural feature of the FeO^{2+} moiety, which determines its activity as an alkane hydroxylation catalyst, is the presence of low-lying acceptor orbitals, namely the $3\sigma^\star$ $3d_{z^2}$–$2p_z$ antibonding orbital. Both the energetic position of this orbital and the spin state of the system (which in turn also affects the $3\sigma^\star$ energy) depend on the surrounding ligands. We present results of density functional theory (DFT) calculations performed on a series of gas-phase complexes of composition $[FeO(H_2O)_n(L)_{5-n}]^{2+}$ (n = 4, 1, 0) derived from the recently characterised aqueous $[FeO(H_2O)_5]^{2+}$ by substitution of ligand water molecules with L = NH_3, CH_3CN, H_2S and BF_3. The calculations reveal that the high-spin (quintet) state is favoured by the weaker σ-donating equatorial ligands, which is consistent with the literature. The high-spin configuration is more reactive because of significant exchange stabilisation of the crucial $3\sigma^\star\uparrow$ orbital. Once the quintet state is formed by a judicious choice of *equatorial* ligands, the reactivity can be fine-tuned by modulating the energy of the $3\sigma^\star$ orbital by varying the nature of the *axial* ligand. A linear relation between the σ-donor properties of the axial ligand (estimated from the magnitude of the orbital interaction between the σ lone pair and the $3\sigma^\star$ orbital) and the activation barrier for the abstraction reaction is observed, and is related to a "push effect" of the σ donors that destabilises the $3\sigma^\star$ orbital. We propose that species with enhanced activation properties for hydrogen abstraction relative to $[FeO(H_2O)_5]^{2+}$ might be obtainable by either replacing the axial ligand with a σ donor weaker than H_2O or by preventing ligands from coordinating to iron in an axial position.

I. Introduction

The identification of high-valent transition-metal-ion intermediates in several enzymatic oxidation processes of biosynthetic and metabolic relevance[1–7] has been one of the key achievements in understanding mechanisms responsible for the in vivo activation and reduction of molecular oxygen. Among the most common cofactors of enzymes involved in oxidative processes, copper, manganese and iron, the latter is by far the most widespread.[8–14] Reactions mediated by iron-containing oxygenases have been studied for over 30 years,[15,16] and high-valent (oxido)Fe^{IV} (ferryl) intermediates were recognised early in compounds I and II of catalases and peroxidases.[17–22] The highly reactive nature of these intermediates hampers their isolation as stable species, and spectroscopic methods, often along with theoretical studies, are thus important sources of information on their structure and mechanistic properties.

High-valent metal states have also been postulated in intermediates of various non-heme-iron–protein catalysed processes. Only recently, however, has the involvement of a ferryl species been conclusively proved, specifically in the catalytic cycle of the taurine/α-ketoglutarate dioxygenase (TauD) enzyme.[23–25] This compound has an S = 2 (quintet) ground state,[26] at variance with the S = 1 (triplet) state invariably observed in model porphyrin and non-porphyrin systems, a fact that has been related to the local geometry of the metal coordination environment.[27] A number of biomimetic polydentate non-heme ligands, such as 1,4,8,11-tetramethyl-1,4,8,11-tetraaza-cyclotetradecane (TMC)[28,29] and *N*,*N*-bis(2-pyridylmethyl)-*N*-bis(2-pyridyl)methylamine (N4Py),[30] capable of stabilising high-valent iron states have been synthesised and extensively studied since 2000.[31,32] Various ferryl complexes with room-temperature lifetimes that range from seconds to days have been generated and identified spectroscopically and, to date, three of them have been characterised crystallographically.[29,31,33,34]

An important issue is the presence and role of different spin states of oxidoiron complexes. The presence of different spin states is a key element in the work on two-state reactivity (mostly of FeO^+) by Schröder, Shaik, Schwarz and co-workers.[35–37] Various computational studies of S = 2 (oxido)Fe^{IV} systems have appeared (e.g. refs.[38–42]). Schöneboom et al.[43] have applied DFT and various correlated ab initio methods to five-coordinate C_{4v} $[FeO]^{2+}$ com-

[a] Theoretische Chemie, Vrije Universiteit Amsterdam,
De Boelelaan 1083, 1081 HV Amsterdam, The Netherlands
Fax: +31-20-598-7629
E-mail: L.Bernasconi@few.vu.nl
EJ.Baerends@few.vu.nl

plexes. In subsequent work,[44] Neese examined in detail the interplay between triplet and quintet states on the structure, energy and spectroscopic properties of $[FeO(NH_3)_5]^{2+}$ by using (hybrid) DFT and multireference configuration interaction methods. The main factor governing the relative stability of the triplet vs. quintet ground state in this simple system was found to be the strength of the equatorial ligand field. The triplet state was found to be lower in energy in the equilibrium geometry having a distance of $R(FeN_{eq})$ = 2.062 Å between the metal centre and the equatorial N atoms, whereas a lower-energy quintet state was found at larger distances [$R(FeN_{eq})$ = 2.203 Å]. Very little influence from the *axial* ligand on the triplet–quintet separation was observed. Furthermore, the length and strength of the Fe^{IV}–O bond was found to be similar for the two spin states. On the basis of DFT calculations, it has also been observed that an S = 1 → S = 2 spin transition would radically change the spectroscopic properties of a $[FeO(TMC)(X)]^{2+}$ species, yet leave the nature of the $Fe^{IV}O$ bond essentially unmodified.[42,45]

Although the S = 1 → S = 2 spin transition has but little effect on the stability of the Fe^{IV}–O bond, this phenomenon has important implications for the *catalytic activity* of $Fe^{IV}O$-containing species. In general, non-heme enzymes (typically S = 2) are more reactive than heme ones (typically S = 1). The fact that in non-heme iron enzymes the metal ion is in a high-spin state while heme enzymes as well as all known synthetic $Fe^{IV}O$ complexes (with the exception of $[FeO(H_2O)_5]^{2+}$) are low-spin[16] is explained by the *weaker ligand field* in the non-heme systems. Although it is well recognised that high-spin complexes are more reactive than the low-spin ones, a straightforward explanation seems to be lacking still; we will address this issue in the present work (cf. also ref.[46]).

Not only the equatorial ligands, but also the axial ligand *trans* to the oxido ligand affects the reactivity. A classical example of the influence of the axial ligand on the activity of metal centres in enzymes is the *push effect* in the dioxygen cleavage reaction catalysed by cytochrome P450,[47–50] to yield the elusive Compound I.[3,13,43,51–53] A strong electron donation from the thiolate ligand in the proximal site of heme was first proposed in 1976[47] to be solely responsible for the highly efficient O–O breaking ability of P450. Although experimental findings have provided some support for this hypothesis,[48,50] a complete model for the catalytic activity of P450 is currently still lacking,[54] and various additional factors (e.g. the presence of potassium ions or specific amino acid residues in the vicinity of the heme site, hydrogen bonds with a proximal cysteine ligand, involvement of a reductase enzyme promoting the electron transfer) may contribute to the regulation of its activity. Isolating and characterising the role of axial ligand effects in the catalytic activity may therefore provide insight into the relative importance of the different factors promoting reactions catalysed by FeO-containing enzymes.

In studying activation effects on hydrogen atom abstraction from weak C–H bonds induced by substitution of the *axial* NCMe with CF_3COO^- in the synthetic S = 1 complex $[FeO(TMC)(NCMe)]^{2+}$, Rohde and Que[28] advanced the hypothesis that this ligand substitution may be able to induce a weakening of the ligand field and provide access to the more reactive S = 2 surface. This study of $[FeO(TMC)(CF_3COO)]^+$, a subsequent one devoted to similar non-heme complexes with anionic ligands, $[FeO(TMC)(NCS)]^+$ and $[FeO(TMC)(N_3)]^+$,[55] and the recent theoretical work of Kamachi et al.,[56] devoted to activation effects in the first step of the cyclohexane hydroxylation reaction induced by anionic ligands coordinated to an $Fe^{IV}O$ porphyrin π-cation radical, confirm the remarkable importance of axial ligands in modulating the activity of oxidoiron complexes in organic oxidations.

$[FeO(H_2O)_5]^{2+}$ has attracted considerable attention from a theoretical perspective, because of its controversial role in the chemistry of the Fenton reaction (oxidation by a mixture of ferrous salts and hydrogen peroxide). The important intermediate in this reaction is either a free hydroxyl radical, as proposed in the 1930s by Haber and Weiss,[57] or the ferryl ion, as proposed by Bray and Gorin.[58]. Ever since, the issue has been the subject of much debate: see the original work of Groves et al.[59,60] and for reviews refs.[15,61–63] and references cited therein. DFT calculations[38,64] and first-principles molecular dynamics[64–66] have shown that the formation of the ferryl ion is thermodynamically favourable in the gas phase and viable in aqueous solution at room temperature. Experimentally, $[FeO(H_2O)_5]^{2+}$ has been obtained by reaction of $[Fe(H_2O)_5]^{2+}$ with O_3 in acidic aqueous solution, and it has been found to be stable over a period of about 10 seconds.[67–69] To date, this is the only known synthetic S = 2 ferryl complex. Buda et al.[38,41] and Louwerse and Baerends[46] presented detailed analyses of the electronic structure of this complex and of the factors governing its reactivity in hydrogen abstraction from methane and methanol. The effect of solvation on reaction barriers was also studied.[46,70,71] The essential results of these studies is that the reactivity of $[FeO(H_2O)_5]^{2+}$ in hydrogen abstraction from a simple alkane or alcohol is a one-electron phenomenon involving the empty $3\sigma^*\uparrow$ orbital of $[FeO(H_2O)_5]^{2+}$, and that solvation affects the reactivity strongly by changing the energy of the latter orbital. The importance of the $3\sigma^*\uparrow$ orbital has also been recognised in the work of Decker et al.[72]

In the present work we analyse the effects of ligand substitution in simple gas-phase systems of composition $[FeO(H_2O)_n(L)_{5-n}]^{2+}$, with L = NH_3, CH_3CN, H_2S and BF_3. As for the precursor species $[FeO(H_2O)_5]^{2+}$, in these systems the metal ion is surrounded by a distorted octahedral coordination environment of C_{2v} symmetry, with four equatorial ligands in roughly planar geometry and one axial ligand in the *trans* position to the oxide ion (Figure 1). The aim of this study is to gauge the relative importance of axial vs. equatorial ligands in: (a) favouring either a low (S = 1) or high (S = 2) spin state; (b) influencing the ability of the system to abstract a hydrogen atom from a methane molecule. We also address the issue of the origin of the higher reactivity in S = 2 vs. S = 1 complexes in alkane hydroxylation.

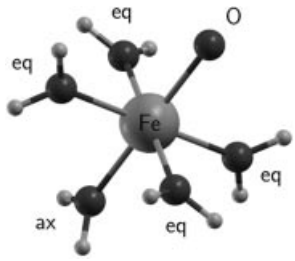

Figure 1. The structure of $[FeO(H_2O)_5]^{2+}$. Equatorial and axial ligands are indicated. O is the O(oxido) atom.

The paper is organised as follows. In Section II, details of the calculations are given. In Section IIIA, we study the role of equatorial and axial ligands in influencing the relative stabilities of high- and low-spin states of the compounds $[FeO(H_2O)_n(NH_3)_{5-n}]^{2+}$. In Section IIIB, we analyse the hydrogen atom transfer reaction from a methane molecule to each of the latter compounds (corresponding to the first step in $Fe^{IV}O$-catalysed aliphatic hydroxylation[15]). We verify the more reactive nature of high-spin complexes, which has experimentally often been observed. Here it is explained as being caused by the strong exchange stabilisation of the crucial $3\sigma^* \uparrow$ acceptor orbital in high-spin complexes with weak equatorial ligand fields. In Section IIIC, we study the manner in which the energy of the latter orbital can be modified by varying the nature of the axial ligand in (high-spin) compounds of composition $[FeO(H_2O)_4(L_{ax})]^{2+}$. The $3\sigma^* \uparrow$ orbital is pushed up by stronger σ donors at the axial coordination site, which leads to reduced reactivity. This effect in the high-spin complexes is opposite to the *push effect* that has been identified in the *low-spin* $Fe^{IV}O$ porphyrin π-cation radical. Our findings are summarised in Section IV. The general rules emerging from our study are, first, that weak-field equatorial ligands are needed to obtain the high-spin state, in order to enhance the good acceptor properties (electrophilic nature) of $[L_5FeO]^{2+}$ through stabilisation of the acceptor orbital, and second, that even higher efficiency of hydrogen atom transfer from methane than in reactions involving $[FeO(H_2O)_5]^{2+}$ might be achievable by occupying the axial coordination site with a weaker donor ligand (or even an electron acceptor), or by leaving it unoccupied and enforcing a square-planar equatorial coordination for iron.

II. Computational Details

Calculations were performed by using ADF[73–75] with a QZ4P basis set for iron and a TZ2P basis set for all other atoms. All electrons were treated explicitly. Relativistic effects were included by using the Zero-Order Regular Approximation (ZORA).[76] In the majority of the calculations exchange-correlation effects were described at the BLYP[77,78] level of theory. Standard generalised gradient corrections (GGAs), as well as the local density approximation, are known to disfavour high-spin states in Fe^{II} and Fe^{III} complexes, as opposed to hybrid and some *meta*-GGA functionals.[79–81] For this reason, in determining the most stable spin state for the ground state of each of the complexes examined, we performed additional full geometry optimisation by using the OPBE functional, a combination of the OPTX[82] and the PBE[83] functionals. OPBE has been shown to yield spin state relative stabilities comparable to hybrid and *meta*-GGA prescriptions.[81,84] Convergence criteria for geometry optimisations were 5×10^{-4} hartree in the total energy, 5×10^{-3} hartree Å^{-1} in the gradients, 5×10^{-3} Å in bond lengths and 0.25° in bond and dihedral angles.

III. Results and Discussion

A. Ligand-Induced Spin Transition in $[FeO(H_2O)_n(NH_3)_{5-n}]^{2+}$

Detailed discussions of the electronic structure of $[FeO]^{2+}$ and of its "microsolvated" counterpart $[FeO(H_2O)_5]^{2+}$ (**1**) are given in refs.[38,41,46,72] The characteristic one-electron spectrum of $[FeO(H_2O)_5]^{2+}$ in its quintet ground state (Figure 2) shows significant stabilisation of the majority of ↑ spin orbitals, caused by the exchange field generated by four unpaired ↑ electrons. For the $d_{xy}\uparrow$ / $d_{xy}\downarrow$ pair, there are additional sources for the especially large gap (see below). Overlap of 3d and O(oxido) 2p orbitals leads to bonding/antibonding pairs of σ symmetry (2σ: $d_{z^2}+p_z$, doubly occupied; $3\sigma^*$: $d_{z^2}-p_z$, virtual) and π symmetry (1π: $d_{xz,yz}+p_{x,y}$, doubly occupied; $2\pi^*$: $d_{xz,yz}-p_{x,y}$, singly occupied). The d orbitals of δ symmetry, $d_{x^2-y^2}$ and d_{xy}, cannot mix by symmetry with O $2p_z$ orbitals, they are one hundred percent d (in FeO^{2+}) and Fe–O nonbonding. The $d_{xy}/d_{x^2-y^2}$ pair with ↑ spin (both singly occupied) are degenerate in bare $[FeO]^{2+}$, but the degeneracy is lifted in the $[FeO(H_2O)_5]^{2+}$ complex by antibonding interactions of the $d_{x^2-y^2}$ orbital with the σ lone pairs of the equatorial water molecules and by bonding interactions of the d_{xy} with their π lone pairs.[41] These contributions bring about a difference in energy of 2.69 eV between the occupied orbitals $d_{xy}\uparrow$ and $d_{x^2-y^2}\uparrow$. The gap between the corresponding unoccupied orbitals $d_{xy}\downarrow$ and $d_{x^2-y^2}\downarrow$ is much smaller (1.13 eV),

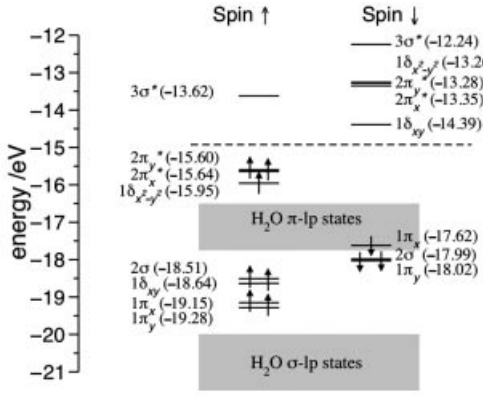

Figure 2. BLYP Kohn–Sham one-particle energies (in parentheses) of $[FeO(H_2O)_5]^{2+}$. The *z* axis is parallel to the Fe–O bond. Shaded areas represent the energy regions spanned by π ($1b_2$) and σ ($2a_1$) lone pairs of the water molecules. The dashed line separates occupied from virtual states (Cf. ref.[46]).

since they are both above the water lone pairs and are both pushed up (only the $d_{xy}\downarrow$ less so by the weaker π interactions than the $d_{x^2-y^2}\downarrow$ by the stronger σ interactions). Nevertheless, the fact that $d_{xy}\uparrow$ is pushed down, on top of being stabilised by the exchange field of the excess ↑ spin electrons, and that the $d_{xy}\downarrow$ is pushed up, on top of being less stabilised by the exchange field, leads to the particularly large gap of 4.25 eV between this ↑/↓ pair. These orbital interactions with the water lone pairs also explain the different nodal structure of the two spin components of the d_{xy} orbital (Figure 3): the $d_{xy}\uparrow$ component, which clearly exhibits the in-phase mixing with water π lone pairs and the $d_{xy}\downarrow$ component, which has out-of-phase mixing with those lone pairs.

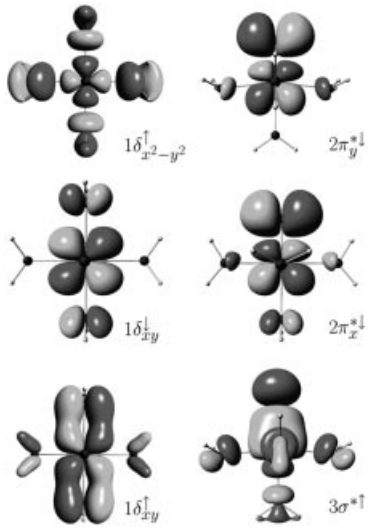

Figure 3. Selected Kohn–Sham orbitals of $[FeO(H_2O)_5]^{2+}$. Nonbonding $1\delta_{x^2-y^2}\uparrow$ and $1\delta_{xy}\downarrow$ orbitals are involved in the composition-induced transition from the quintet to the triplet ground state, in which they act as the donor and acceptor of one electron, respectively. Antibonding $2\pi_{x,y}^*\downarrow$ and $3\sigma^*\uparrow$ orbitals, which are empty in both spin states, regulate the attitude of the $Fe^{IV}O$ towards accepting electrons from a substrate and determine the reaction pathway in H-atom abstraction from a hydrocarbon. In the three plots on the left, the *z* axis [parallel to the Fe–O(oxido) bond] is perpendicular to the plane of the page, and the axial water molecule is not visible. In the plots on the right, the *z* axis is along the vertical and the axial ligand is in the lower part of each plot.

We consider now the substitution of the ligand water molecules with ammonia molecules to yield axially monosubstituted $[FeO(H_2O)_4(NH_3)]^{2+}$ (**1a**), equatorially substituted $[FeO(NH_3)_4(H_2O)]^{2+}$ (**1b**) and the fully ammoniated complex $[FeO(NH_3)_5]^{2+}$ (**1c**). The Kohn–Sham levels for these complexes are shown in Figure 4. The monosubstituted complex **1a** was found to possess a quintet ground state, albeit the difference in energy between quintet and triplet was found to decrease in comparison to the all-water complex **1** (Table 1). In accordance with ref.,[81] we found the BLYP functional to underestimate the absolute value of the quintet–triplet energy difference as compared to OPBE. The two did, however, yield a ground state with the same multiplicity in all complexes. For **1b** and **1c**, the triplet state appears to be preferred, although the difference in energy between the two spin states, particularly in the fully ammoniated system, is small. So, we find here that, in agreement with the results of ref.[44], the spin state of the complex is almost completely determined by the nature of the equatorial ligands: electron donating ligands in the equatorial position favour the low-spin triplet state.

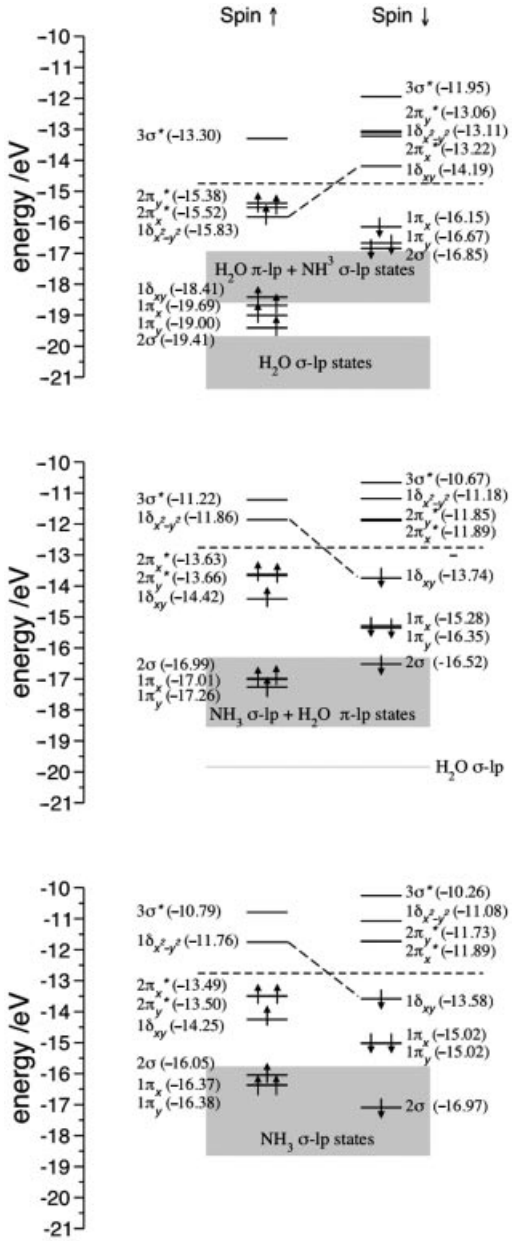

Figure 4. Kohn–Sham energy levels of axially (*top*), equatorially (*centre*) and fully NH_3-substituted $[FeO(H_2O)_n(NH_3)_{5-n}]^{2+}$ (n = 4, 1, 0) complexes. The first system is in a quintet ground state, the second and third in a triplet. Oblique dashed lines indicate the energy difference between $1\delta_{x^2-y^2}\uparrow$ and $1\delta_{xy}\downarrow$ orbitals. See main text for details.

The reason is simple. Equatorial substitution selectively affects the energy of orbitals extending in the *xy* plane. Since the σ lone pair of NH_3 is more electron-donating than

Table 1. Second and third columns: differences between quintet (S = 2) and triplet (S = 1) ground state energies of $[FeO(H_2O)_n(NH_3)_{5-n}]^{2+}$. The data refer to fully optimised geometries for each spin state. Fourth through eighth column: BLYP energies of selected Kohn–Sham spin orbitals in the ground state with the most stable spin multiplicity (S = 2 for **1** and **1a**, S = 1 for **1b** and **1c**). *o* and *e* indicate occupied and empty orbitals, respectively. Note the change in occupations in going from **1a** to **1b**. All values are in eV.

		BLYP	OPBE	$1\delta_{x^2-y^2}\uparrow$	$2\pi_x^*\uparrow$	$2\pi_y^*\uparrow$	$1\delta_{xy}\downarrow$	$3\sigma^*\uparrow$
1	$[FeO(H_2O)_5]^{2+}$	–0.280171	–1.131758	–15.95 *o*	–15.64 *o*	–15.60 *o*	–14.39 *e*	–13.62 *e*
1a	$[FeO(H_2O)_4(NH_3)]^{2+}$	–0.206509	–0.697896	–15.83 *o*	–15.52 *o*	–15.38 *o*	–14.19 *e*	–13.30 *e*
1b	$[FeO(H_2O)(NH_3)_4]^{2+}$	0.523687	0.139269	–11.86 *e*	–13.63 *o*	–13.66 *o*	–13.74 *o*	–11.22 *e*
1c	$[FeO(NH_3)_5]^{2+}$	0.443386	0.049770	–11.76 *e*	–13.49 *o*	–13.50 *o*	–13.58 *o*	–10.79 *e*

the σ lone pair of H_2O, an orbital like $d_{x^2-y^2}$ with antibonding σ interactions with the ligands is strongly destabilised, and the $d_{x^2-y^2}\uparrow$ moves in the orbital spectrum close to the $3\sigma^*\uparrow$ orbital (Figure 5). It actually becomes so high-lying that it loses its electron to the empty, now lower-lying ↓ spin orbital $d_{xy}\downarrow$. It should be noted that the effect of equatorial NH_3 substitution is different for the d_{xy} orbitals of ↑ and ↓ spin. The $d_{xy}\uparrow$ loses the pushing down effect of the higher-lying π lone pairs of the equatorial waters and moves up, like $d_{x^2-y^2}\uparrow$ did; the $d_{xy}\downarrow$ loses the pushing up effect of the lower-lying water π lone pairs and moves down, so that it even more readily accepts the electron of the destabilised $d_{x^2-y^2}\uparrow$ orbital. Electron transfer from $d_{x^2-y^2}\uparrow$ to $d_{xy}\downarrow$ entails a spin flip, with the effect that the stabilising exchange field for the ↑ spin orbitals becomes smaller, which provides an additional relative destabilisation of $d_{x^2-y^2}\uparrow$ with respect to $d_{xy}\downarrow$. This spin flip leaves only two unpaired ↑ spin electrons in the $2\pi^*$ orbitals, hence a triplet state. We note that finally the $d_{xy}\uparrow$ and $d_{xy}\downarrow$, which are both occupied, have now a much reduced gap (ca. 0.7 eV) relative to the initial gap of 4.2 eV. The remaining gap reflects the remaining exchange stabilisation of the two excess ↑ spins in the $2\pi^*$ orbitals. Since electron transfer from the $d_{x^2-y^2}\uparrow$ to the $d_{xy}\downarrow$ orbital occurs between orbitals with nonbonding Fe–O character, the stability of the $Fe^{IV}O$ bond is barely affected.[42,44,45] This is confirmed by the change in the $Fe^{IV}O$ bond length of no more than ≈0.02 Å as a function of composition and/or spin state (Table 2). The spin flip has, nevertheless, a crucial effect on the reactivity, because of the loss of (part of) the exchange stabilisation of the $3\sigma^*\uparrow$ orbital. The role of the $3\sigma^*\uparrow$ orbital in the reactivity is discussed in the following sections.

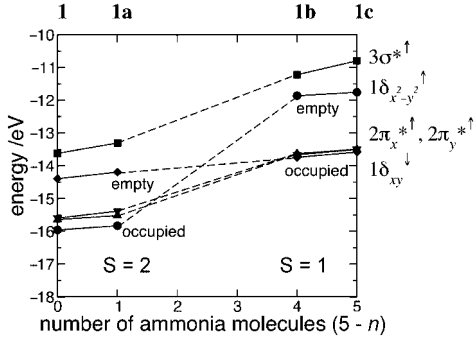

Figure 5. Energy of selected spin orbitals of $[FeO(H_2O)_n(NH_3)_{5-n}]^{2+}$ as a function of the number of ammonia molecules, 5–*n*, in the complex. Lines are guides for the eye.

Substitution of only the axial water molecule in **1** with ammonia has a very moderate destabilising effect (upshift of 0.1–0.3 eV) for all orbitals of π and δ symmetry (Figure 5), consistent with the fact that their wavefunctions have zero overlap with the σ lone pair of the axial NH_3. Replacement of the axial water molecule with ammonia does, however, more visibly affect orbitals with lobes along the *z* axis (the Fe–O bond axis) like 2σ, which is pushed down by the higher-lying NH_3 lone pair by ca. 1 eV, and the $3\sigma^*$ orbital, which is pushed up by ca. 0.3 eV. In fact, the overall orbital energy pattern is little affected by substitution of only the axial water molecule, and this substitution is not in itself able to induce a transition from high- to low-spin multiplicity, although a destabilisation of the S = 2 state vs. S = 1 is observed, possibly caused by small changes in the geometry of the equatorial ligand environment (Table 2). In either spin state, the effects of axial ligands on the energy

Table 2. Selected bond lengths [Å] in $[FeO(H_2O)_n(NH_3)_{5-n}]^{2+}$ (*n* = 5, 4, 1, 0) complexes. All geometries have been optimised in both high- and low-spin states. Subscripts ax and eq refer to ligands in axial and equatorial positions, respectively. For equatorial distances, averages over four values are reported.

		$\langle O_{eq}–Fe\rangle$		$O_{ax}–Fe$		$\langle N_{eq}–Fe\rangle$		$N_{ax}–Fe$		Fe–O	
		S = 1	S = 2	S = 1	S = 2	S = 1	S = 2	S = 1	S = 2	S = 1	S = 2
1	$[FeO(H_2O)_5]^{2+}$	2.000	2.106	2.117	2.091	–	–	–	–	1.627	1.621
1a	$[FeO(H_2O)_4(NH_3)]^{2+}$	2.018	2.121	–	–	–	–	2.173	2.147	1.641	1.636
1b	$[FeO(H_2O)(NH_3)_4]^{2+}$	–	–	2.215	2.153	2.079	2.232	–	–	1.633	1.627
1c	$[FeO(NH_3)_5]^{2+}$	–	–	–	–	2.087	2.244	2.221	2.173	1.647	1.641

of the 3σ* orbital (pushing up by stronger donors) will have a similar effect on the reactivity. This will be discussed in Section III C. Overall, the S = 2 → S = 1 spin conversion upon equatorial NH_3 substitution has the effect of raising the axial 3σ* ↑ orbital away from the vicinity of the Fermi energy. This fact will be shown to bear remarkable consequences on the electron-acceptor properties of the coordinated $[FeO]^{2+}$ group.

B. Ligand Effects on Hydrogen Abstraction from Methane

Alkane hydroxylation by the $[Fe^{IV}O]^{2+}$ species follows a *rebound mechanism*.[15,59,60,70] First, one hydrogen atom is abstracted from the substrate to yield $[Fe^{III}OH]^{2+}$ and a carbon radical. The latter then collapses onto the hydroxy oxygen. It has been emphasised that the ability of $[Fe^{IV}O]^{2+}$ to promote hydrogen abstraction is directly connected to its electrophilic character: the FeO···HR bond is established by electron donation out of the RH bonding orbitals into a low-lying acceptor orbital on $[Fe^{IV}O]^{2+}$.[46,72] The empty 3σ* ↑ orbital lies 2 eV above the HOMO $2\pi_x$* ↑ and 0.3 eV below the next occupied $2\pi_x$* ↓ orbital, and it has a lobe extending on the oxygen side of the $Fe^{IV}O$ group (Figure 3). Its energy and shape thus make it an ideal acceptor for the electron of the incoming hydrogen atom. Its unusual stability, in spite of being an antibonding Fe $3d_{z^2}$–O $2p_z$ combination, originates (apart from the 2+ charge on FeO^{2+} and the stabilising exchange field in particular in the high-spin state) from an in-phase overlap of O $2p_z$ with the equatorial torus of the Fe $3d_{z^2}$. This contribution attenuates the antibonding character of the orbital (cf. Figure 5 in ref.[46]). Analysis of the interaction between $[FeO(H_2O)_5]^{2+}$ and various substrate molecules (CH_4, CH_3OH, H_2O) has indeed shown that the 3σ* ↑ orbital plays a cardinal role in driving hydrogen abstractions in the gas phase, in aqueous solution and possibly in other media.[46] In all these cases, the abstraction reaction was found to follow an identical pattern, involving as first step the formation of a $[FeO(H_2O)_5]^{2+}$–substrate encounter complex. The bonding energy of the complex, ranging from 9 (CH_4) to 70 (CH_3OH) kJ mol^{-1}, reflects the amount of interaction between the donor orbital (HOMO) of the substrate and the 3σ* ↑ orbital of $[FeO(H_2O)_5]^{2+}$. In the case of methane, the in-phase combination of one of the T_2 molecular orbitals and the latter has 89% T_2 and 11% 3σ* ↑ character. This situation corresponds to a partial, if small, transfer of an electron from the donor to the acceptor. In the more tightly bound methanol complex, the mixing of donor and 3σ* ↑ in their bonding combination is 55–45%, indicating that the electron is almost equally shared between the donor orbital and the 3σ* ↑ orbital. In both the methane and methanol complexes, the donor orbital is essentially a C–H σ bond. Partial promotion of an electron to the 3σ* ↑ orbital thus results in a weakening of this bond. Since the overall reaction brings about the net transfer of one electron from the substrate to $[FeO(H_2O)_5]^{2+}$ via a concerted bond breaking (substrate–H) and bond formation (H–OFe^{IV}),[15] partial electron transfer in the reactants corresponds to a starting electronic structure more similar to the transition state, hence to a lower activation barrier. The stronger the electron-sharing interaction between the substrate molecule and $[FeO(H_2O)_5]^{2+}$ in the encounter complex, the more facile is then the abstraction of the hydrogen atom from the substrate.

We show in Figure 6 the abstraction barriers for the reaction of CH_4 with the axially, equatorially and fully ammoniated complexes **1a**, **1b**, **1c**. The energy of the 3σ* ↑ orbital is 0.32 (in **1a**), 2.4 (in **1b**) and 2.8 eV (in **1c**) higher than that in the nonammoniated complex **1** (Table 1). These complexes are representative of (a) an S = 2 system (the complex **1a**) with moderate 3σ* ↑ destabilisation (as compared to the all-water complex **1**), and (b) two S = 1 systems (the complexes **1b** and **1c**) with large and comparable 3σ* ↑ destabilisation. Reaction profiles were obtained by (unconstrained) preliminary optimisation of the encounter complex followed by constrained reduction of the O(oxido)–H distance. For each value of the constraint, a full geometry optimisation was carried out. The reaction barrier for hydrogen abstraction is defined here as the difference in total energy between the transition state (at the maximum of each curve) and the energy of the reactant complex. We computed barriers of 54, 111 and 103 kJ mol^{-1} for **1a** + CH_4, **1b** + CH_4 and **1c** + CH_4, respectively. These should be compared to the value for the **1** + CH_4 abstraction reaction, 23 kJ mol^{-1}.[46] Overall, a decrease in the reaction rate is therefore observed in the sequence **1** > **1a** > **1b** ≈ **1c**.

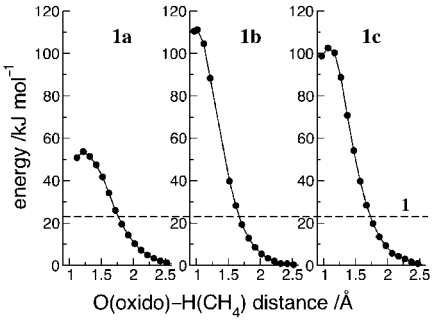

Figure 6. Energy barriers for C–H bond cleavage in axially (**1a**), equatorially (**1b**) and fully (**1c**) NH_3-substituted $[FeO(H_2O)_5]^{2+}$. The total energy of the $[FeO(H_2O)_n(NH_3)_{5-n}]^{2+} + CH_4$ complex is represented here as a function of the constrained O(oxido)–H distance. The energy of the reactant complex is taken as the zero point of the energy scale. The dashed line indicates the barrier height for $[FeO(H_2O)_5]^{2+}$ (**1**, see ref.[46]).

The transition to the triplet ground state as a result of equatorial substitution (i.e. going from **1** to **1b**) raises the height of the barrier roughly by a factor of four. Substitution of the axial water molecule, both in **1** and **1b** has, by contrast, only a moderate effect. This trend mirrors the moderate destabilisation of the 3σ* ↑ orbital, 0.3 eV (**1** → **1a**) and 0.4 eV (**1b** → **1c**), to be compared to the much larger effect of equatorial substitution and spin flip, e.g.

2.5 eV for **1a** → **1c**. We do, however, observe that, although the destabilisation of the 3σ*↑ orbital is moderate in both **1** → **1a** and **1b** → **1c**, the latter substitution (axial ligand) results in a much larger increase in the reaction barrier. This is the only case in which no correlation is observed between 3σ*↑ energy and reaction barrier, and this indicates that in triplet compounds the reactivity is no longer *exclusively* determined by the 3σ*↑ orbital alone. The ability of the 3σ*↑ orbital to act as an electron accepting orbital (AO) depends in the first place on its energy relative to the donating orbital (DO) of the substrate. The energy of AO and the DO should be compared in the same conditions (geometry, overall charge, etc.) as in the starting reactant complex. A second factor contributing to the AO–DO interaction is the spatial distribution of the 3σ*↑ orbital. Since the electron transfer occurs at the oxygen side of the Fe–O group and the 3σ*↑ orbital arises from a combination of the Fe $3d_{z^2}$ and the $2p_z$ orbital of O(oxido), the large contribution from the latter (ca. 50%) results in enhanced in-phase overlap of 3σ*↑ with the DO.

For a given substrate, the variation of the energy of the 3σ*↑ orbital in the $[L_5FeO]^{2+}$ complex caused by ligand replacement or other environmental changes provides a qualitative index of reactivity. An upward shift of the 3σ*↑ orbital results in larger activation barriers. The changes that induce a rise in the orbital energy of 3σ*↑ lead to a concomitant reduction of the amplitude of the 3σ*↑ orbital at the oxido side. Axial substitution pushes the $3d_{z^2}$ up directly, and equatorial substitution does so indirectly by causing a spin flip and a weaker exchange field. The relative contributions of the Fe $3d_{z^2}$ to the AO 3σ*↑ therefore increase along the sequence **1** → **1a** → **1b** → **1c**, varying as 37%, 42%, 52%, 51%, and those of the O(oxido) $2p_z$ diminish in the sequence 48%, 30%, 25%, 23%, respectively. So there is a progressive localisation of the orbital on the metal centre and a consequent decrease in the ability to overlap with the DO on the O(oxido) side. Both factors, the higher orbital energy of the 3σ*↑ orbital and the decreasing amplitude at the oxido side, work in the same direction in increasing the activation barrier.

We observe that this model, using only the 3σ*↑ AO and the C–H bonding orbital as the DO, applies strictly only to those FeO^{2+} complexes in which 3σ*↑ is the only important acceptor orbital. This only holds for a quintet ground state. The S = 2 → S = 1 transition not only destabilises 3σ*↑, decreasing its electron accepting ability, but it also opens an alternative electron-transfer channel through the now lower lying $2\pi_x$*↓ and $2\pi_y$*↓ orbitals (Figure 5, **1b** and **1c**). An incoming DO might then interact with the 3σ*↑ and $2\pi_{x,y}$*↓ orbitals simultaneously, leading to an Fe–O–H angle that is considerably smaller than the 180° we have observed in the quintet state.[46] The proximity of the empty $2\pi_{x,y}$*↓ orbitals even in the quintet state, will make the energy surface of the reactant complex, and probably also that of the transition state, rather flat with respect to the Fe–O–H angle.

C. Axial Ligand Influence on Reactivity

We showed in the previous sections that: (1) the spin state of a complex $[FeO(L_{eq})_4(L_{ax})]^{2+}$ is determined by the nature of the equatorial ligands (L_{eq}) alone; (2) the quintet ground state is more reactive than the triplet in hydrogen abstractions; (3) the reactivity of the quintet ground state is driven by the transfer of an electron to a low-lying 3σ*↑ orbital; (4) the axial ligand (L_{ax}) regulates the reactivity of the complex by inducing relatively minor (few tenths of an eV) shifts in the energy of the 3σ*↑ orbital. Here we address the issue of how the last effect can be directed to tuning the reactivity of an Fe^{IV}–O complex in C–H bond cleavage.

We examined a series of simple systems $[FeO(H_2O)_5]^{2+}$, by substitution of either the axial or the equatorial ligand water molecules with CH_3CN and H_2S, but carrying the same charge. Similar to the $[FeO(H_2O)_n(NH_3)_{5-n}]^{2+}$ complexes described above, a transition to a triplet ground state was observed for $L_{eq} = CH_3CN$, irrespective of the nature of L_{ax}. The situation is far less clear in the H_2S-substituted complexes, where differences in energy between the quintet and triplet states after equatorial substitution are within 0.02 eV. In both CH_3CN and H_2S complexes, however, replacement of only the axial ligand was not sufficient to favour the triplet over the quintet state, similar to NH_3 substitution, OPBE quintet–triplet energy differences being ≈0.4 and ≈0.2 eV in the CH_3CN and H_2S complexes respectively. In particular, we observed an overall change of no more than ≈0.2 eV in the energy difference between $1\delta_{xy}$↓ and $1\delta_{x^2-y^2}$↑ as a result of the replacement of the axial ligand (Table 3).

Replacement of the axial ligand in $[FeO(H_2O)_4(L_{ax})]^{2+}$ was found to decrease slightly the energy of the 3σ*↑ orbital in the case of H_2S (–0.06 eV) and to increase it by 0.72 eV in the case of CH_3CN. The relative 3σ*↑ contri-

Table 3. BLYP Kohn–Sham orbital energies (in eV) for optimised complexes of composition $[FeO(H_2O)_4(L_{ax})]^{2+}$, where L_{ax} indicates the axial ligand. Values for $[FeO(H_2O)_5]^{2+}$ are from ref.[46]

	$1\delta_{x^2-y^2}$↑	$2\pi_x$*↑	$2\pi_y$*↑	3σ*↑	$1\delta_{xy}$↓	$1\delta_{x^2-y^2}$↓	$2\pi_x$*↓	$2\pi_y$*↓
$[FeO(H_2O)_5]^{2+}$	–15.95	–15.64	–15.60	–13.62	–14.39	–13.26	–13.35	–13.28
$[FeO(H_2O)_4(NH_3)]^{2+}$	–15.83	–15.52	–15.38	–13.30	–14.19	–13.11	–13.22	–13.06
$[FeO(H_2O)_4(H_2S)]^{2+}$	–15.70	–15.54	–14.85	–13.68	–14.27	–13.12	–13.32	–13.25
$[FeO(H_2O)_4(CH_3CN)]^{2+}$	–15.23	–15.07	–15.07	–12.90	–13.66	–12.57	–12.84	–12.83
$[FeO(H_2O)_4(BF_3)]^{2+}$	–16.15	–16.03	–15.98	–14.13	–14.58	–13.44	–13.71	–13.65
$[FeO(H_2O)_4(o)]^{2+}$	–16.64	–16.64	–16.48	–14.78	–15.19	–13.91	–14.32	–14.13

bution to the in-phase $3\sigma^* \uparrow -e_z$ orbital combination is very similar in the H_2O and H_2S complexes (11 and 10% respectively) as well as in the CH_3CN and NH_3 complexes (both 7%). C–H cleavage reaction barriers vary according to the sequence $[FeO(H_2O)_4(H_2S)]^{2+} \approx [FeO(H_2O)_5]^{2+} < [FeO(H_2O)_4(CH_3CN)]^{2+} < [FeO(H_2O)_4(NH_3)]^{2+}$. This mirrors the total amount of $3\sigma^* \uparrow -e_z$ orbital interaction in the reactant complex and, to a lesser extent, the absolute energy of the $3\sigma^* \uparrow$ orbital. The initial $3\sigma^* \uparrow -e_z$ orbital interaction is a good index of reactivity, since in all complexes the transition state is characterised by an equal distribution of the electron between the DO and the AO (Table 4), which will be obtained more readily if the starting point is more strongly mixed. The overall height of the activation barrier is therefore correlated with the contribution of the $3\sigma^* \uparrow$ orbital to the CH_4–$[FeO(H_2O)_4(L_{ax})]^{2+}$ charge-transfer state; the larger this quantity the lower the activation energy.

Table 4. Percentage $3\sigma^* \uparrow$ character in the in-phase $3\sigma^* \uparrow -e_z$ overlap for methane complexes ($3\sigma^* \uparrow$ %) in the reactant complex (RC) and transition state (TS) geometries. Percentage contribution of σ lone pair (or e_1 in $[FeO(H_2O)_4(BF_3)]^{2+}$ to $3\sigma^* \uparrow$ (Ax σ-lp). C–H bond-cleavage barrier (ΔE_{TS}, in kJ mol^{-1}) for hydrogen abstraction from CH_4. Values for $[FeO(H_2O)_5]^{2+}$ are from ref.[46]

	$3\sigma^* \uparrow$ %		Ax σ-lp%	ΔE_{TS}
	RC	TS		
$[FeO(H_2O)_5]^{2+}$	11	46	1.71	23
$[FeO(H_2O)_4(NH_3)]^{2+}$	7	52	4.95	54
$[FeO(H_2O)_4(H_2S)]^{2+}$	10	49	1.94	25
$[FeO(H_2O)_4(CH_3CN)]^{2+}$	7	49	3.06	41
$[FeO(H_2O)_4(BF_3)]^{2+}$	25	54	<1	7
$[FeO(H_2O)_4(o)]^{2+}$	34	48	0	1

We have verified that a stronger σ-donating axial ligand decreases the ability of a $[FeO(H_2O)_4(L_{ax})]^{2+}$ complex to promote C–H bond breaking, and that a ligand with a σ-donating character comparable to that of water (H_2S) leaves it virtually unchanged.[85] It is therefore reasonable to expect that a ligand with no σ-donor character might be able to revert the trend in reactivity observed above and yield an even higher reactivity than that obtained with all-water ligands. For this reason we studied the compound $[FeO(H_2O)_4(BF_3)]^{2+}$, where as before the electron-deficient BF_3 ligand occupies the axial position. Although this species was found to be stable in the gas phase, we do not address here the issue of its stability either with respect to $[FeO(H_2O)_5]^{2+}$ or as a solvated species. The BF_3 molecule coordinates to the metal centre through one of the fluorine atoms with a Fe–F–B angle of 141.1°. The $3\sigma^* \uparrow$ orbital (Figure 7) exhibits a nodal structure analogous to the one observed in $[FeO(H_2O)_5]^{2+}$; one of the B–F bonding orbitals of BF_3 replaces the σ lone pair of H_2O, and its energy is 0.51 eV lower than that in the latter species. For this system, we computed a C–H dissociation barrier of only 7 kJ mol^{-1}, which is consistent with the large $3\sigma^* \uparrow$ stabilisation.

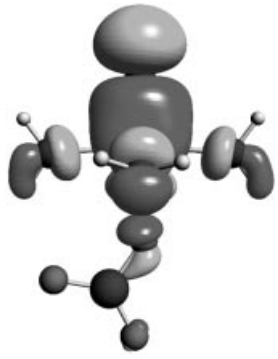

Figure 7. The $3\sigma^* \uparrow$ orbital in $[FeO(H_2O)_4(BF_3)]^{2+}$. The BF_3 molecule axially coordinated to Fe^{IV} is in the lower portion of the figure. The orientation is as in Figure 3, right column. Note that the C_3 axis of the BF_3 ligand is not perpendicular to the z axis, and one of the B–F bonds is roughly oriented toward the metal centre.

Finally, we consider a hypothetical $[FeO(H_2O)_4(o)]^{2+}$ complex in which the axial ligand is removed, and the O–Fe–O angles (where O stands for the oxygen atoms of the remaining ligands) are constrained to their values as in $[FeO(H_2O)_5]^{2+}$. Owing to the absence of an antibonding combination with orbitals of the axial ligand, the energy of the $3\sigma^* \uparrow$ orbital is further lowered relative to the BF_3 complex to 1.16 eV below its value in $[FeO(H_2O)_5]^{2+}$. The C–H bond cleavage occurs with virtually no barrier, the activation energy being lower than 1 kJ mol^{-1}. In the reactant complex, the DO of CH_4 carries a substantial $3\sigma^* \uparrow$ character (34%, vs. 53% e_z character), which is roughly three times as much as that in the $[FeO(H_2O)_5]^{2+} + CH_4$ complex.

In Figure 8 we show activation barriers as a function of the percentage σ lone pair character of the axial ligand (or the e_1 orbital in the case of BF_3) in the $3\sigma^* \uparrow$ orbital. The latter quantity can be taken as measure of the overall "push" (or destabilisation) experienced by the $3\sigma^* \uparrow$ orbital because of the presence of a σ-donating ligand. For the S = 2 complexes considered in this work, this quantity varies from 0 (for $[FeO(H_2O)_4(o)]^{2+}$) to 4.95% (for $[FeO(H_2O)_4(NH_3)]^{2+}$), and the C–H activation barriers are shown here to depend on it linearly (with a correlation coefficient ≈0.98).

It is interesting to observe that Rohde and Que[28] have found that the axial NCMe ligand in $[FeO(TMC)(L_{ax})]^{2+}$ leads to lower reactivity than the axial carboxylate ligand CF_3COO^-. These are low-spin complexes because of equatorial nitrogen donor coordination by the TMC ligand, and the carboxylate substitution may, as suggested by the authors, lead to relative stabilisation of the high-spin S = 2 state, so that the latter becomes more easily accessible (possibly along the reaction path, in a two-state reactivity process). We do indeed find the difference between the S = 1 ground state and the S = 2 state in **1c** to be very small (BLYP) or vanishing (OPBE). However, we should note that the experimental observation corresponds to the expected effect of a weaker ligand field from the carboxylate than from the NCMe ligand, leading to reduced destabilisa-

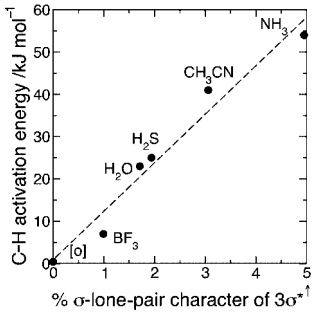

Figure 8. C–H bond-cleavage energy as a function of percentage σ lone pair contribution to the 3σ*↑ orbital in isolated $[FeO(H_2O)_4(L_{ax})]^{2+}$ complexes. The nature of L_{ax} is indicated, and [o] represents the complex with removed axial ligand. The dashed line (with slope 11.47 kJ mol^{-1} and intercept 0.89 kJ mol^{-1}) has been obtained by linear regression from the calculated values.

tion of the 3σ*↑ orbital. Overall, the activation effect observed in ref.[28] is therefore fully consistent with the molecular orbital model of reactivity described here.

IV. Conclusions

We have highlighted the electronic structural features explaining the extraordinary reactivity of the $[Fe^{IV}O]^{2+}$ group in the oxidation of aliphatic C–H bonds: (a) a very low-lying acceptor orbital interacts with the C–H bonding orbital which acts as a donor; (b) in high-spin complexes, the energy of the 3σ*↑ acceptor orbital is lowered by the exchange field of the excess ↑ spin electrons, leading to enhanced reactivity.

The empty 3σ*↑ orbital ($3d_{z^2}$–$2p_z$) is the most important acceptor orbital, being low-lying and having a large amplitude at the oxido ligand. We have detailed that the non-bonding electrons in the dδ orbitals $3d_{x^2-y^2}$ and $3d_{xy}$ (perpendicular to the Fe–O axis) are not just spectator electrons. When a ligand-induced switching occurs from the unpaired spin electron configuration $(3d_{x^2-y^2}\uparrow)^1(3d_{xy}\uparrow)^1$ to the spin-paired configuration $(3d_{xy})^2$, the lowering of the spin multiplicity from S = 2 to S = 1 makes the exchange field of the unpaired spin up electrons considerably less stabilising, and the empty 3σ*↑ shifts up. It then less readily accepts electrons from the C–H bonding orbital, hence the low-spin state S = 1 will require a higher activation energy in the hydrogen abstraction step. The spin state is determined by the ligand environment, in particular by the equatorial ligand field acting on the $d_{x^2-y^2}$ orbital. We analysed a series of compounds of composition $[FeO(L_{eq})_4(L_{ax})]^{2+}$ derived from $[FeO(H_2O)_5]^{2+}$ (S = 2) by substitution of water with ligands with enhanced or decreased σ-donor capability. For all complexes, there are two possible ground states of different spin multiplicity (quintet or triplet) lying close in energy. The quintet ground state was found to be more stable for $[FeO(H_2O)_5]^{2+}$ and all the systems in which only the axial water molecule is replaced. The triplet ground state is favoured by the stronger σ-donating ligands (e.g. $L_{eq} = NH_3$). These ligands push the $3d_{x^2-y^2}\uparrow$ up, so that it becomes favourable for it to shed its electron into the originally empty $3d_{xy}\downarrow$, where it can pair up with the electron in the $3d_{xy}\uparrow$.

Whereas the equatorial ligands have the most important effect, determining the spin state, the *axial* ligand (*trans* to the oxido ligand) directly interacts with the crucial acceptor orbital 3σ*↑ and affects its energy and shape. Therefore, the catalytic properties can be fine-tuned by varying the σ-donor properties of the *axial* ligand alone. Changes in the orbital energy of ≈1 eV or less may result in variations of up to 100 kJ mol^{-1} in the C–H bond cleavage activation barrier. We also proved that axial ligands with decreased σ-donor ability enhance the catalytic properties of $[FeO(H_2O)_5]^{2+}$-derived systems by decreasing the energy of the 3σ*↑ orbital and favouring its overlap with a suitable donor orbital of the substrate. We also proved the existence of a linear relation between the magnitude of the mixing between 3σ*↑ and the axial-ligand orbital responsible for its destabilisation. The effect of the *axial* ligand can be optimally tuned by modifying its σ-donor properties. In the absence of σ donation (as in the hypothetical $[FeO(H_2O)_4(o)]^{2+} + CH_4$ system), C–H bond cleavage occurs almost spontaneously.

In summary, the optimal electronic properties for C–H bond activation and hydroxylation require a high-spin state, which is favoured by equatorial ligands with a weak ligand field, such as H_2O. A weak axial ligand field is similarly favourable, once the high-spin state is stabilised by a suitable equatorial field. These findings are consistent with the high catalytic activity of non-heme enzymes with flexible ligand environments and oxygen donor ligands rather than nitrogen lone pairs, such as TauD. The 2-His 1-carboxylate facial triad in the active site of the latter system consists of an equatorial ligand set with one nitrogen donor; the other equatorial ligands are oxygen based (e.g. H_2O). The remaining histidine ligand coordinates the metal centre through a nitrogen donor in the axial site, a situation that is, according to our analysis, not optimal. A carboxylate ligand instead of a nitrogen donor in the axial position would in principle be more favourable, which is also in accordance with the results of ref.[28] The insights gained in this work may be helpful in devising catalytic species for homogeneous alkane hydroxylation with superior activation properties, as well as in understanding the mechanistic role of oxidation intermediates containing high-valent metal centres with $[FeO(H_2O)_5]^{2+}$-like coordination and supported by a protective framework, such as zeolites[86] and oxygenated EDTA–Fe complexes in aqueous solution.[87–89]

Acknowledgments

This work was supported by the Dutch National Research School Combination "Catalysis by Design" (NRSC-C). Computer resources were provided by the Netherlands' Scientific Research Council (NOW) through a grant from the Stichting Nationale Computerfaciliteiten (NCF).

[1] A. Ghosh, *J. Inorg. Biochem.* **2006**, *100*, 419–420.
[2] G. T. Babcock, *Proc. Natl. Acad. Sci. USA* **1999**, *96*, 12971–12973.
[3] T. Omura, *Biochem. Biophys. Res. Com.* **1999**, *266*, 690–698.
[4] W. L. Smith, D. L. DeWitt, R. M. Garavito, *Annu. Rev. Biochem.* **2000**, *69*, 145–182.
[5] F. D'Agnillo, A. I. Alayash, *Free Radical Biol. Med.* **2002**, *33*, 1153–1164.
[6] R. K. Behan, M. T. Green, *J. Inorg. Biochem.* **2006**, *100*, 448–459.
[7] A. V. Nemukhin, I. A. Topol, R. E. Cachau, S. K. Burt, *Theor. Chem. Acc.* **2006**, *115*, 348–353.
[8] A. L. Feig, S. J. Lippard, *Chem. Rev.* **1994**, *94*, 759–805.
[9] L. Que Jr, R. Y. N. Ho, *Chem. Rev.* **1996**, *96*, 2607–2624.
[10] B. J. Wallar, J. D. Lipscomb, *Chem. Rev.* **1996**, *96*, 2625–2657.
[11] E. I. Solomon, T. C. Brunold, M. I. Davis, J. N. Kemsley, S.-K. Lee, N. Lehnert, F. Neese, A. J. Skulan, Y.-S. Yang, J. Zhou, *Chem. Rev.* **2000**, *100*, 235–349.
[12] T. D. H. Bugg, *Tetrahedron* **2003**, *59*, 7075–7101.
[13] I. G. Denisov, T. M. Makris, S. G. Sligar, I. Schlichting, *Chem. Rev.* **2005**, *105*, 2253–2277.
[14] S. Shaik, D. Kumar, S. P. de Visser, A. Altun, W. Thiel, *Chem. Rev.* **2005**, *105*, 2279–2328.
[15] J. T. Groves, *J. Inorg. Biochem.* **2006**, *100*, 434–447.
[16] A. Bassan, M. R. A. Blomberg, T. Borowski, P. E. M. Siegbahn, *J. Inorg. Biochem.* **2006**, *100*, 727–743.
[17] P. G. Debrunner, *Hyperfine Interact.* **1990**, *53*, 21–36.
[18] R. Rutter, M. Valentine, M. P. Hendrich, L. P. Hager, P. G. Debrunner, *Biochemistry* **1983**, *22*, 4769–4774.
[19] R. Rutter, L. P. Hager, H. Dhonau, M. Hendrich, M. Valentine, P. Debrunner, *Biochemistry* **1984**, *23*, 6809–6816.
[20] C. E. Schulz, P. W. Devaney, H. Winkler, P. G. Debrunner, N. Doan, R. Chiang, R. Rutter, L. P. Hager, *FEBS Lett.* **1979**, *103*, 102–105.
[21] C. E. Schulz, R. Rutter, J. T. Sage, P. G. Debrunner, L. P. Hager, *Biochemistry* **1984**, *23*, 4743–4754.
[22] H.-P. Hersleth, U. Ryde, P. Rydberg, C. H. Görbitz, K. K. Andersson, *J. Inorg. Biochem.* **2006**, *100*, 460–476.
[23] J. C. Price, E. W. Barr, B. Tirupati, J. M. Bollinger Jr, C. Krebs, *Biochemistry* **2003**, *42*, 7497–7508.
[24] J. C. Price, E. W. Barr, T. E. Glass, C. Krebs, J. M. Bollinger Jr, *J. Am. Chem. Soc.* **2003**, *125*, 13008–13009.
[25] D. A. Proshlyakov, T. F. Henshaw, G. R. Monterosso, M. J. Ryle, R. P. Hausinger, *J. Am. Chem. Soc.* **2004**, *126*, 1022–1023.
[26] P. J. Riggs-Gelasco, J. C. Price, R. B. Guyer, J. H. Brehm, E. W. Barr, J. M. Bollinger Jr, C. Krebs, *J. Am. Chem. Soc.* **2004**, *126*, 8108–8109.
[27] C. Krebs, J. C. Price, J. Baldwin, L. Saleh, M. T. Green, J. M. Bollinger Jr, *Inorg. Chem.* **2005**, *44*, 742–757.
[28] J.-U. Rohde, L. Que Jr, *Angew. Chem. Int. Ed.* **2005**, *44*, 2255–2258.
[29] J.-U. Rohde, J.-H. In, M. H. Lim, W. W. Brennessel, M. R. Bukowski, A. Stubna, E. Münck, W. Nam, L. Que Jr, *Science* **2003**, *299*, 1037–1039.
[30] J. Kaizer, E. J. Klinker, N. Y. Oh, J.-U. Rohde, W. J. Song, A. Stubna, J. Kim, E. Münck, W. Nam, L. Que Jr, *J. Am. Chem. Soc.* **2004**, *126*, 472–473.
[31] X. Shan, L. Que Jr, *J. Inorg. Biochem.* **2006**, *100*, 421–433.
[32] M. M. Conradie, J. Conradie, A. Ghosh, *J. Inorg. Biochem.* **2006**, *100*, 620–626.
[33] E. J. Klinker, J. Kaizer, W. W. Brennessel, N. L. Woodrum, C. J. Cramer, L. Que Jr, *Angew. Chem. Int. Ed.* **2005**, *44*, 3690–3694.
[34] M. R. Bukowski, K. D. Koehntop, A. Stubna, E. L. Bominaar, J. A. Halfen, E. Münck, W. Nam, L. Que Jr, *Science* **2005**, *310*, 1000–1002.
[35] N. Harris, S. Shaik, D. Schröder, H. Schwarz, *Helv. Chim. Acta* **1999**, *82*, 1784–1797.
[36] S. Shaik, M. Filatov, D. Schröder, H. Schwarz, *Chem. Eur. J.* **1998**, *4*, 193–199.
[37] D. Schröder, S. Shaik, H. Schwarz, *Acc. Chem. Res.* **2000**, *33*, 139–145.
[38] F. Buda, B. Ensing, M. C. M. Gribnau, E. J. Baerends, *Chem. Eur. J.* **2001**, *7*, 2775–2783.
[39] A. Ghosh, E. Tangen, H. Ryeng, P. R. Taylor, *Eur. J. Inorg. Chem.* **2004**, *23*, 4555–4560.
[40] A. Bassan, M. R. A. Blomberg, P. E. M. Siegbahn, *Chem. Eur. J.* **2003**, *9*, 106–115.
[41] F. Buda, B. Ensing, M. C. M. Gribnau, E. J. Baerends, *Chem. Eur. J.* **2003**, *9*, 3436–3444.
[42] A. Decker, J.-U. Rohde, L. Que Jr, E. I. Solomon, *J. Am. Chem. Soc.* **2004**, *126*, 5378–5379.
[43] J. C. Schöneboom, F. Neese, W. Thiel, *J. Am. Chem. Soc.* **2005**, *127*, 5840–5853.
[44] F. Neese, *J. Inorg. Biochem.* **2006**, *100*, 716–726.
[45] N. Lehnert, R. Y. N. Ho, L. Que Jr, E. I. Solomon, *J. Am. Chem. Soc.* **2001**, *123*, 8271–8290.
[46] M. J. Louwerse, E. J. Baerends, *Phys. Chem. Chem. Phys.* **2007**, *9*, 156–166.
[47] J. H. Dawson, R. H. Holm, J. R. Trudell, G. Barth, R. E. Linder, E. Bunnenberg, C. Djerassi, S. C. Tang, *J. Am. Chem. Soc.* **1976**, *98*, 3707–3709.
[48] J. H. Dawson, M. Sono, *Chem. Rev.* **1987**, *87*, 1255–1276.
[49] J. H. Dawson, *Science* **1988**, *240*, 433–439.
[50] M. Sono, M. P. Roach, E. D. Coulter, J. H. Dawson, *Chem. Rev.* **1996**, *96*, 2841–2887.
[51] T. M. Makris, K. von Koenig, I. Schlichting, S. G. Sligar, *J. Inorg. Biochem.* **2006**, *100*, 507–518.
[52] V. Guallar, R. A. Friesner, *J. Am. Chem. Soc.* **2004**, *126*, 8501–8508.
[53] A. Altun, V. Guallar, R. A. Friesner, S. Shaik, W. Thiel, *J. Am. Chem. Soc.* **2006**, *128*, 3924–3925.
[54] C. Limberg, *Angew. Chem. Int. Ed.* **2003**, *42*, 5932–5954.
[55] C. V. Sastri, M. J. Park, T. Ohta, T. A. Jackson, A. Stubna, M. S. Seo, J. Lee, J. Kim, T. Kitagawa, E. Münck, L. Que Jr, W. Nam, *J. Am. Chem. Soc.* **2005**, *127*, 12494–12495.
[56] T. Kamachi, T. Kouno, W. Nam, K. Yoshizawa, *J. Inorg. Biochem.* **2006**, *100*, 751–754.
[57] F. Haber, J. Weiss, *Naturwiss.* **1932**, *51*, 948–950.
[58] W. C. Bray, M. H. Gorin, *J. Am. Chem. Soc.* **1932**, *54*, 2124–2125.
[59] J. T. Groves, M. Van Der Puy, *J. Am. Chem. Soc.* **1974**, *96*, 5274–5275.
[60] J. T. Groves, G. A. McClusky, *J. Am. Chem. Soc.* **1976**, *98*, 859–861.
[61] P. Wardman, L. P. Candeias, *Radiat. Res.* **1996**, *145*, 523–531.
[62] H. B. Dunford, *Coord. Chem. Rev.* **2002**, *233*, 311–318.
[63] F. Gozzo, *J. Mol. Catal. A* **2001**, *171*, 1–22.
[64] B. Ensing, F. Buda, P. Blöchl, E. J. Baerends, *Phys. Chem. Chem. Phys.* **2002**, *4*, 3619–3627.
[65] B. Ensing, F. Buda, P. Blöchl, E. J. Baerends, *Angew. Chem. Int. Ed.* **2001**, *40*, 2893–2895.
[66] B. Ensing, E. J. Baerends, *J. Phys. Chem. A* **2002**, *106*, 7902–7910.
[67] T. Løgager, J. Holcman, K. Sehested, T. Pedersen, *Inorg. Chem.* **1992**, *31*, 3523–3529.
[68] O. Pestovsky, A. Bakac, *J. Am. Chem. Soc.* **2004**, *126*, 13757–13764.
[69] O. Pestovsky, S. Stoian, E. L. Bominaar, X. Shan, E. Münck, L. Que Jr, A. Bakac, *Angew. Chem. Int. Ed.* **2005**, *44*, 6871–6874.
[70] B. Ensing, F. Buda, M. C. M. Gribnau, E. J. Baerends, *J. Am. Chem. Soc.* **2004**, *126*, 4355–4365.
[71] M. J. Louwerse, P. Vassilev, E. J. Baerends, *J. Phys. Chem. A*, submitted.
[72] A. Decker, M. D. Clay, E. I. Solomon, *J. Inorg. Biochem.* **2006**, *100*, 697–706.
[73] *ADF2005.01*, SCM, Theoretical Chemistry, Vrije Universiteit Amsterdam, The Netherlands; http://www.scm.com.
[74] E. J. Baerends, D. E. Ellis, P. Ros, *Chem. Phys.* **1973**, *2*, 41–51.

[75] C. Fonseca Guerra, J. G. Snijders, G. te Velde, E. J. Baerends, *Theor. Chem. Acc.* **1998**, *99*, 391–403.
[76] E. van Lenthe, E. J. Baerends, J. G. Snijders, *J. Chem. Phys.* **1994**, *101*, 9783–9792.
[77] A. Becke, *Phys. Rev. A* **1988**, *38*, 3098–3100.
[78] C. Lee, W. Yang, R. G. Parr, *Phys. Rev. B* **1988**, *37*, 785–789.
[79] A. Fouqueau, S. Mer, M. E. Casida, L. M. L. Daku, A. Hauser, T. Mineva, F. Neese, *J. Chem. Phys.* **2004**, *120*, 9473–9486.
[80] A. Fouqueau, M. E. Casida, L. M. L. Daku, A. Hauser, F. Neese, *J. Chem. Phys.* **2005**, *122*, 044110.
[81] M. Swart, A. R. Groenhof, A. W. Ehlers, K. Lammertsma, *J. Phys. Chem. A* **2004**, *108*, 5479–5483.
[82] N. C. Handy, A. J. Cohen, *Mol. Phys.* **2001**, *99*, 403–412.
[83] J. P. Perdew, K. Burke, M. Ernzerhof, *Phys. Rev. Lett.* **1996**, *77*, 3865–3868.
[84] A. R. Groenhof, M. Swart, A. W. Ehlers, K. Lammertsma, *J. Phys. Chem. A* **2005**, *109*, 3411–3417.
[85] As previously observed, the preference for a quintet ground state is not as marked in $[FeO(H_2O)(H_2S)]^{2+}$ as it is in $[FeO(H_2O)_5]^{2+}$. In practice, this factor may hamper the catalytic activity of the former system.
[86] G. I. Panov, A. K. Uriarte, M. A. Rodkin, V. I. Sobolev, *Catal. Today* **1998**, *41*, 365–385.
[87] T. Mizuta, J. Wang, K. Miyoshi, *Inorg. Chim. Acta* **1995**, *230*, 119–125.
[88] S. Seibig, R. van Eldik, *Inorg. Chem.* **1997**, *36*, 4115–4120.
[89] L. Bernasconi, E. J. Baerends, in preparation.

Received: December 22, 2006
Published Online: May 10, 2007

